



# Modeling of flow boiling heat transfer coefficient of R11 in mini-channels using support vector machines and its comparative analysis with the existing correlations

Nusrat Parveen<sup>1</sup> · Sadaf Zaidi<sup>1</sup> · Mohammad Danish<sup>1</sup>

Received: 24 March 2018 / Accepted: 20 August 2018 / Published online: 14 September 2018  
© Springer-Verlag GmbH Germany, part of Springer Nature 2018

## Abstract

In recent years, extensive research efforts have been devoted to flow boiling heat transfer mechanisms in macro and mini-channels. However, it is still difficult to predict the flow boiling heat transfer coefficient with satisfactory accuracy. In this study, support vector regression (SVR) models have been constructed using a respectable experimental database (767 samples) from the literature to predict the heat transfer coefficient of R11 in mini-channels for subcooled (324 samples) and saturated (443 samples) boiling regions. The prediction performance of the SVR-based models have been evaluated based on the statistical parameters. SVR-based models have been found to exhibit an average absolute relative error (AARE) of 1.7% and correlation coefficient (R) of 0.9996 for subcooled boiling, while for saturated boiling the values of AARE and R are 1.6% and 0.9993, respectively. Also, the developed SVR-based models have been compared with the well-known existing correlations. The superior prediction performance of SVR-based models has been observed with the lowest value of AARE and the highest value of correlation coefficient (R). Furthermore, parametric effects of mass flux, vapor quality, heat flux and pressure on the flow boiling heat transfer coefficient have also been investigated and the SVR-based models have been found to agree well with the experimental results.

## Nomenclature

$B_o$	Boiling number
$C$	Cost function
$Co$	Convective number
$C_p$	Specific heat, J/kg.K
$D_h$	Hydraulic diameter, m
$f(x)$	Regression function
$G$	Mass flux, kg/m <sup>2</sup> .s
$h$	Heat transfer coefficient, kW/m <sup>2</sup> .K
$h_{ig}$	Enthalpy of vaporization, J/kg
$k$	Thermal conductivity, W/m.K
$K(x_i, x_j)$	Kernel function
$L$	Dual form of the Lagrangian function
$P$	Fluid pressure, kPa
$Pe$	Peclet number
$Pr$	Prandtl number
$Q^2_{ext}$	Leave-one-out cross validation for the test set

$Q^2_{Loo}$	Leave-one-out cross validation for the training set
$R$	Correlation coefficient
$Re$	Reynolds number
$S$	Suppression factor
$T$	temperature, K
$q$	heat flux density, W/m <sup>2</sup>
$x_i$	Input vector
$X_{tt}$	Lockhart-Martinelli parameter
$y_i$	Output vector

## Subscripts

$l$	Liquid phase
$nb$	Nucleate boiling
$sat$	Saturated
$tp$	Two-phase
$v$	Vapor phase
$w$	Wall

## Greek symbols

$\Gamma$	Surface development parameter
$\sigma$	Width parameter of RBF kernel
$\varepsilon$	Loss function
$\gamma$	Regularization parameter
$\lambda$ and $\lambda^*$	Lagrange multipliers
$\phi(x_i)$	High dimensional mapping feature function for input vector $x$
$K$	Thermal conductivity, W/m.K

✉ Sadaf Zaidi  
s.zaidi.ke@amu.ac.in; sadaf63in@yahoo.com

<sup>1</sup> Department of Chemical Engineering, Z.H. College of Engineering and Technology, Aligarh Muslim University, Aligarh, UP 202002, India

$\mu$	Kinematic viscosity, kg/m.s
$\rho$	Density, kg/m <sup>3</sup>
$\sigma$	Surface tension, N/m

### Abbreviations

AARE	Average absolute relative error
ANN	Artificial neural network
MRE	Mean relative error
RBF	Radial basis function
SVM	Support vector machines
SVR	Support vector regression
SRM	Structural risk minimization
RMSE	Root mean square error
SD	Standard deviation

## 1 Introduction

Trichlorofluoromethane, R11 was supposed to be the first widely used refrigerant as low-pressure centrifugal chillers. R-11 is a non-corrosive, non-toxic, and non-flammable refrigerant. Its low operating pressures and relatively high compressor displacement require the use of a centrifugal compressor. Selection of refrigerant based on initial and operating costs, system design, size, safety, reliability, serviceability etc. is important for applications such as microprocessor cooling, cooling of high power electronic equipment, compact heat exchangers, and even compact fuel cells. Even though its use has been discontinued in recent days due to its high ozone depleting potential but enormous amount of experimental data is available in literature that help to understand the mechanism of flow boiling in mini-channels. In the present work, a part of this data has been used to assess the applicability of SVR to

predict the heat transfer coefficient in mini-channels for both the subcooled as well as the nucleate boiling regions. Future work would entail the use of data on eco-friendly refrigerants to develop more robust soft computing models. Based on the hydraulic diameter, the flow channels have been grouped into the conventional macro-channels, micro-channels and mini-channels as follows [1–4]:

- Conventional channels:  $D_h \geq 3$  mm
- Mini-channels:  $3 \text{ mm} \geq D_h > 200 \mu\text{m}$
- Micro-channels:  $200 \mu\text{m} \geq D_h > 10 \mu\text{m}$

Flow boiling heat transfer in mini-channels has attracted the interest of many researchers. The use of mini and micro-channels with suitable fluid could provide high heat transfer; reduce the cost of material and save space. It has been found from the literature that the flow boiling is governed by both nucleate boiling and forced convective heat transfer mechanisms. The heat transfer coefficient in nucleate boiling regime is mainly dependent upon heat flux and mass velocity and vapor quality has negligible effect on heat transfer coefficient while in the forced convection boiling dominant regime, the heat transfer coefficient has been found to be dependent on mass velocity and vapor quality, and is less sensitive to heat flux [5]. Furthermore, the forced convection boiling region is usually related to the annular flow pattern, and the nucleate boiling region with the bubbly and slug flow patterns [6, 7]. So, mass velocity, vapor quality, and heat flux, and flow pattern help in recognizing the dominant heat transfer mechanism in a micro-channel/mini-channel.

A good design of heat transfer equipment requires accurate prediction of flow boiling heat transfer coefficient, as this

**Fig. 1** The representation of SVM for regression problem using  $\epsilon$ -insensitive loss function

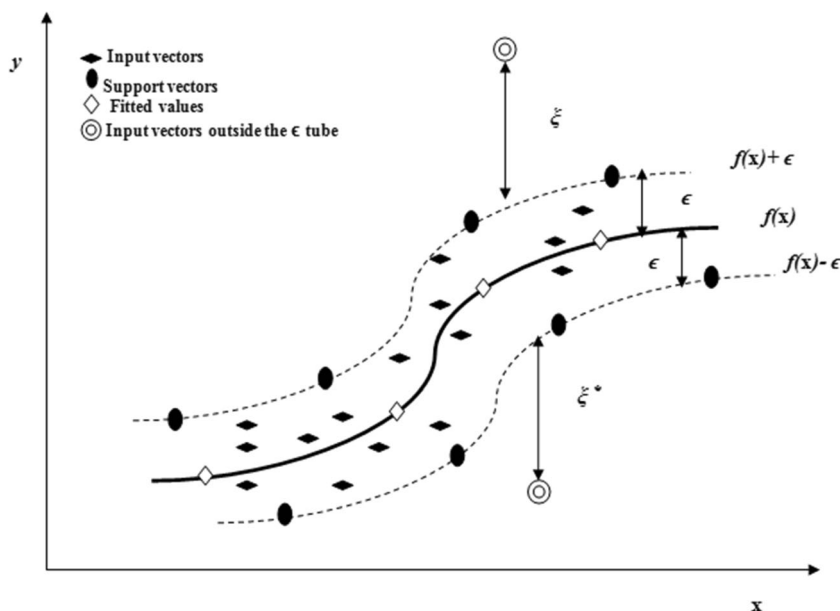


**Table 1** Flow boiling heat transfer correlations

Authors	Correlations	Fluids/Parameters Range
Chen [34]	$h_{tp} = S \cdot h_{nb} + F \cdot h_{sp}$ $F = \begin{cases} 2.35 \left( \frac{1}{X_{tt}} + 0.213 \right)^{0.736} & \text{if } 1/X_{tt} > 0.1 \\ 1 & \text{if } 1/X_{tt} \leq 0.1 \end{cases}$ $S = 1 / (1 + 2.53 \cdot 10^{-6} Re_l^{1.17})$ $X_{tt} \left( \frac{1-x}{X} \right)^{0.9} \left( \frac{\rho_l}{\rho_g} \right)^{0.5} \left( \frac{\mu_l}{\mu_g} \right)^{0.1}$ $Re = \frac{(1-x)G_p D_h}{\mu_l}$ $h_{nb} = 0.00122 \left( \frac{k_l^{0.79} c_{p,l}^{0.45} \rho_l^{0.49}}{\sigma^{0.5} \mu_l^{0.29} h_{lg}^{0.24} \rho_g^{0.24}} \right) \Delta T_{sat}^{0.24} \Delta P_{sat}^{0.75}$	Vertical flow; water, methanol, cyclohexane, pentane, benzene; P: 1–34.8 bar q: 6.2–2400 Kw/m <sup>2</sup> x: 0.01–0.71
Gungor & Winterton [35]	$h_{tp} = (SS_2 + FF_2)h_{sp}$ Where, $h_{sp} = 0.023 Re_l^{0.8} Pr_l^{0.4} k_l / D_h$ $Re_l = \frac{(1-x)G_p D_h}{\mu_l}$ $Pr_l = \frac{C_p \mu_l}{k_l}$ $S = 1 + 3000 Bo^{0.86}$ $F = 1.12 \left( \frac{x}{1-x} \right)^{0.75} \left( \frac{\rho_l}{\rho_g} \right)^{0.41}$ $S_2 = \begin{cases} Fr_{lo}^{(0.1-2Fr_{lo})} & \text{if horizontal } Fr_{lo} < 0.05 \\ 1 & \text{otherwise} \end{cases}$ $Bo = q / (G_p \cdot h_{lg})$ $Fr_{lo} = \frac{G_p^2}{g D \rho_l^3}$	Vertical and horizontal flow; R-11, R-12, R-22, R-113, R-114, ethylene glycol and water; D: 2.95–32 mm m: 67–61,518 kg/m <sup>2</sup> s P: 0.08–202.6 bar q: 1.1–2280 kW/m <sup>2</sup> x: 0–1
Kandlikar [36]	$h_{tp} = \text{larger} \left\{ \frac{h_{tp,nb}}{h_{tp,cb}} \right.$ $h_{tp,nb} = [0.6683 Co^{-0.2} f(Fr_{lo}) + 1058.0 Bo^{0.7} F_f] (1-x)^{0.8} h_{lo}$ $h_{tp,cb} = [1.136 Co^{-0.9} f(Fr_{lo}) + 667.2 Bo^{0.7} F_f] (1-x)^{0.8} h_{lo}$ $f(Fr_{lo}) = \begin{cases} 1 & \text{for } Fr_{lo} \geq 0.04 \\ (25 Fr_{lo})^{0.3} & \text{for } Fr_{lo} < 0.4 \end{cases}$ $Co = \left( \frac{1-x}{X} \right)^{0.8} \left( \frac{\rho_g}{\rho_l} \right)^{0.5}$ $h_{lo} = \frac{(f/8) Re_{lo} Pr_l (k_l/D)}{1 + 12.7 (f/8)^{1/4} (Pr_l^{1/4} - 1)}$ $f = (0.79 \ln Re_{lo} - 1.64)^{-2}$	Vertical and horizontal flow; water, R-11, R-12, R-114, nitrogen, neon; Bo: 0:03*10 <sup>-4</sup> –46.5*10 <sup>-4</sup> D: 4–32 mm G: 13–8179 kg/m <sup>2</sup> s P: 0.4–64.2 bar q: 0.3–2280 kW/m <sup>2</sup> x: 0.001–0.987
Lazarek & Black [37]	$h_{tp} = 30 Re_{lo}^{0.857} Bo^{0.714} \frac{k_l}{D_h}$ $Re_{lo} = \frac{G_p D_h}{\mu_l}$ $Bo = q / (G_p \cdot h_{lg}); x : < 0-0.60$	R113 Bo: 2.3*10 <sup>-4</sup> –76*10 <sup>-4</sup> D: 3.1 mm G: 125–750 kg/m <sup>2</sup> s Re: 860–5500 P: 1.3–4.1 bar q: 14–380 kW/m <sup>2</sup>
Lee & Mudawar [38]	$h_{tp} = 3.856 X^{0.267} h_l \text{ for } 0 \leq x \leq 0.05$ $h_{tp} = 436.48 Bo^{0.522} We_l^{0.351} X^{0.665} h_l \text{ for } 0.05 < x \leq 0.55$ $h_{tp} = \text{Max} (108.6 X^{1.665} h_g, h_g) \text{ for } 0.055 < x \leq 1$	Water, R134a D: 0.35 mm G: 127–654 kg/m <sup>2</sup> s P: 1.44–6.6 bar q: 159–938 kw/m <sup>2</sup>
Liu & Winterton [39]	$h_{tp}^2 = (Sh_{nb})^2 + (Fh_{sp})^2$ $F = 0.35 \left[ 1 + x Pr_l \left( \frac{\rho_l}{\rho_g} \right) \right]$ $S = \frac{1}{(1 + 0.055 F^{0.1} Re^{0.16})}$ $h_{sp} = 0.023 Re_l^{0.8} Pr_l^{0.4} k_l / D_h$	D: 2.95–32.0 mm G: 12.4–8179.3 kg/m <sup>2</sup> s Re: 568.9–8.75*10 <sup>5</sup> q: 0.35–2620 kW/m <sup>2</sup> Pr: 0.0023–0.895 x: 0–0.948

**Table 1** (continued)

Authors	Correlations	Fluids/Parameters Range
Shah [40]	$h_{nb} = 55P_R^{0.12}(-0.4343 \ln P_R)^{-0.55}q^{0.67}$ $h = 230Bo^{0.67}h_{io}$	Vertical and horizontal flow; water, R-11, R-12, R-22, R-113, cyclohexane; D: 1.1–27.1 mm G: 10–11,071 kg/m <sup>2</sup> s Pr: 0.004–0.8 q: 0.2–1250 kW/m <sup>2</sup> x: 0–0.95
Warrier et al. [41]	$h_{tp} = [1 + 6Bo^{1/16} - 5.3(1 - 855Bo)x^{0.65}]h_{sp}$ .....Saturated boiling $h_{tp} = [1 + 6Bo^{1/16} + 290(1 - 855Bo)Sc^{4.15}]h_{sp}$ .....Subcooled boiling $h_{sp} = 0.023 Re_l^{0.8} Pr_l^{0.4} k_l / D_h$ x: 0.03–0.5	FC-84 0.00027 ≤ Bo ≤ 0.00089 0.03 ≤ x ≤ 0.55 D: 0.75 mm G: 557–1600 kg/ s m <sup>2</sup> q: 59.9 kW/m <sup>2</sup>
Piasecka [42]	$h = 22.5 \Gamma (PeBo)^{0.64} We^{0.46} k / D_h$ .....Saturated boiling $h = 52 \Gamma^{-4} (PeBo)^{0.53} We^{0.12} k / D_h$ .....Subcooled boiling	FC-72 0.14 ≤ x ≤ 0.48 0.028 < Γ < 0.032 Saturated boiling FC-72, R-123, R-11 411 ≤ Re <sub>l</sub> ≤ 4730 0 < Γ < 0.032 Subcooled boiling

parameter is responsible for the surface area and thereby the weight and cost of the equipment. A number of correlations in the literature can be found for the prediction of flow boiling heat transfer coefficient [8–11]. But these correlations have some limitations for their range of applicability under different operating conditions. Olayiwola and Ghiaasiaan [12, 13] have also applied and tried to predict the flow boiling heat transfer coefficient with the several existing correlations using the dataset available in the literature [14–16]. They have found that the performance of each correlation is different for a different dataset, and none of the correlations could provide an accurate prediction of all the three datasets. In the recent past, support vector machines (SVMs) have been adapted for regression. Support vector regression (SVR), a data-driven modeling technique is able to map causal factors and consequent outcomes from the observed patterns (experimental data), without deep knowledge of the complex physical process and this modeling technique is now becoming popular among engineers. Moreover, it offers a lot of advantages over the traditional existing techniques like artificial neural networks (ANN) in the sense that SVM gives a unique, optimal and global solution for the quadratic programming problem, and only two parameters need to be selected: upper bound and kernel parameter. This is because of the structural risk minimization (SRM) principle of SVM which provides good generalization performance. Two more advantages of SVMs are that they have a simple geometric interpretation and give a sparse solution. SVMs find use in many applications such as

in predicting the thermal-hydraulic performance of compact heat exchangers [17], prediction of circulation rate in thermosiphon reboilers [18], streamflow forecasting [19], landslide prediction [20], time series prediction [21], pharmaceutical data analysis [22], prediction of heavy metal removal efficiency from waste water [23, 24] etc. Its excellent prediction performance to many real world problems has motivated the authors to apply SVR for the modeling of both saturated and subcooled boiling of R11 in mini-channels. To the best of the authors' knowledge, there is no published literature available on the application of support vector regression (SVR) for modeling of flow boiling processes in mini-channels. It is for the first time that SVR has been applied to predict the heat transfer coefficient of R11 in mini-channels.

In this study, SVR-based models have been developed and validated for both subcooled and saturated boiling with the experimental data available from the literature of boiling flow using the refrigerant R-11 [14]. Furthermore, the results obtained from the developed SVR-based models have been compared with those obtained from several existing correlations. The SVR-based models have shown a high degree of agreement with the experimental results.

## 2 Abridged theory of SVR-based modeling

SVM theory in detail can be well understood from various works in the literature [25–28]. SVR-based models do not suffer

**Table 2** Optimal parameters for the SVR-based model for predicting the subcooled flow boiling heat transfer coefficient

Model	C	$\gamma = 1/2\sigma^2$	$\epsilon$	Kernel type	Type of loss function	Number of support vectors	Number of training points
Heat transfer coefficient, $h$	32,600	0.029	0.01	RBF	$\epsilon$ - insensitive	145	259

from over-fitting problems i.e. high accuracy for training dataset and low for test dataset (unseen) as they are based on the SRM principle which always guarantees a unique, global and optimal solution. SVR-based models do not rely on the amount of data. Even with a fewer amount of data, they can give a good prediction. However, the only disadvantage of using SVR technique is that it requires optimization of the model and kernel parameters to give excellent prediction with higher accuracy i.e. SVR-based parameter needs to be optimized via some optimization

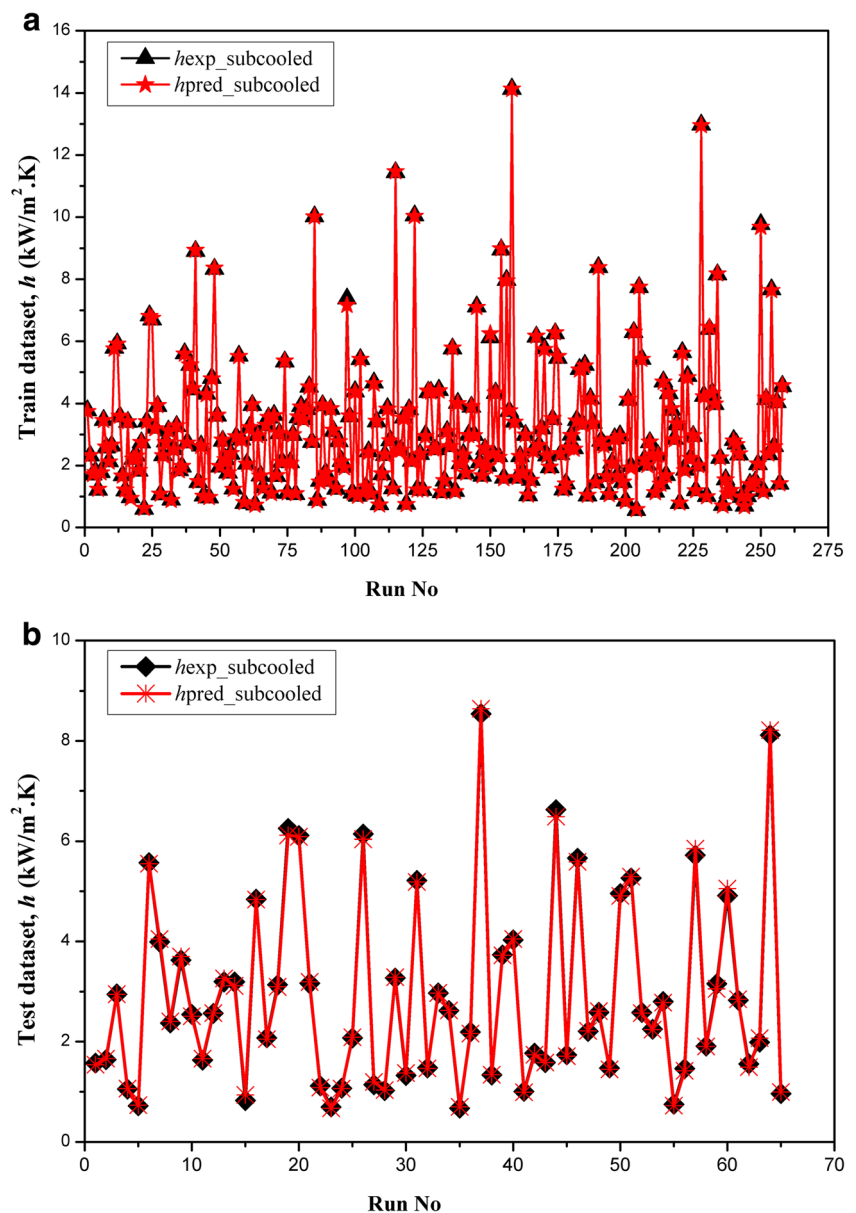
techniques like grid search methodology with 10-fold cross-validation, genetic algorithm (GA), particle swarm optimization (PSO), differential evolution (DE) etc.

In  $\epsilon$ -SVR regression, a function is fitted so as to correctly predict the outputs  $y_i$  for a new set of independent input variables,  $x_i$ . Training dataset for a typical regression problem is as follows:

$$\{(x_1, y_1) \dots (x_n, y_n)\} \subset X \times \mathfrak{R} \quad (1)$$

where  $x$  denotes the space of the input patterns.

**Fig. 2** **a** Training course curve for predicting the subcooled flow boiling heat transfer coefficient,  $h$ . **b** Test course curve for predicting the subcooled flow boiling heat transfer coefficient,  $h$



The regression function in the feature space can be estimated as:

$$f(x, w) = (w \bullet \phi(x) + b) \tag{2}$$

where,  $f$  is termed as feature function and  $w \bullet \phi(x)$  as the dot product in the high dimensional feature space, F. SVR first maps the input data into high dimensional feature space with a non-linear mapping function.

The regularized risk function is minimized to compute the coefficients as given below:

$$R(f) = \frac{1}{2} \|w\|^2 + C \frac{1}{N} \sum_{i=1}^N L_\epsilon(y, f(x, w)) \tag{3}$$

where, the first term of this equation is the model flatness and the second term represents the empirical or training error and is calculated by  $\epsilon$ -insensitive loss function as proposed by Vapnik [29] given as:

$$L_\epsilon(y, f(x, w)) = \begin{cases} 0 & \text{if } |y - f(x, w)| \leq \epsilon \\ |y - f(x, w)| - \epsilon & \text{otherwise} \end{cases} \tag{4}$$

The regularization parameter  $C$  is a trade-off between the empirical or training error and flatness of the model. Slack variables  $\xi$  and  $\xi^*$  are introduced to measure the deviation larger than  $\epsilon$  as demonstrated in Fig. 1 and the expression for SVR can be mathematically given using Eq. (5):

$$\begin{aligned} \text{Minimize} \quad & \frac{1}{2} \|w\|^2 + C \sum_{i=1}^N \xi_i + \xi_i^* \\ \text{Subject to} \quad & (y_i - w \bullet \phi(x) - b) \leq \epsilon + \xi_i \\ & (w \bullet \phi(x) + b - y_i) \leq \epsilon + \xi_i^* \\ & \xi_i, \xi_i^* \geq 0 \end{aligned} \tag{5}$$

Transforming Eq. (5) into the dual form using Lagrange multipliers,  $\lambda$  and  $\lambda^*$  and the final form is given as:

**Table 3** SVR-based evaluation indices based on statistical parameters for subcooled boiling

Model Evaluation Indices for Subcooled Boiling	Train data	Test data
AARE (%)	0.81	1.71
R	0.99993	0.9996
RMSE	0.0109	0.0244
SD	1.8953	2.1585
MRE	0.0081	0.0168
$Q^2_{\text{LOO}}$ (Train data), $Q^2_{\text{ext}}$ (Test data)	0.9998	0.9992

$$f(x, \lambda_i, \lambda_i^*) = \sum_{i=1}^{N_{SV}} (\lambda_i - \lambda_i^*) (\phi(x_i) \bullet \phi(x_j)) + b \tag{6}$$

The solution of Eq. (6) gives the values of the Lagrange multipliers,  $\lambda$  and  $\lambda^*$ . But, only those input vectors,  $x_i$  with non-zero coefficients of  $\lambda$  and  $\lambda^*$  are the support vectors (SVs).

As the dimensions in the input space increase, the computation in the feature space becomes cumbersome which is called as the curse of dimensionality. So, to avoid this, kernel functions are employed [30]. Kernel functions transform the input space data into a linear representation in the high dimensional feature space, thereby facilitating all the computations to be carried out implicitly in the input space instead of in the feature space [31, 32]. This is called the kernel trick and the kernel function has the following form:

$$K(x_i, x_j) = (\phi(x_i) \bullet \phi(x_j)) \tag{7}$$

Moreover, a kernel function must satisfy the Mercer’s condition i.e. it should be symmetric, and positive semi-definite

**Fig. 3** SVR simulation for predicting the subcooled flow boiling heat transfer coefficient,  $h$  using optimal parameters

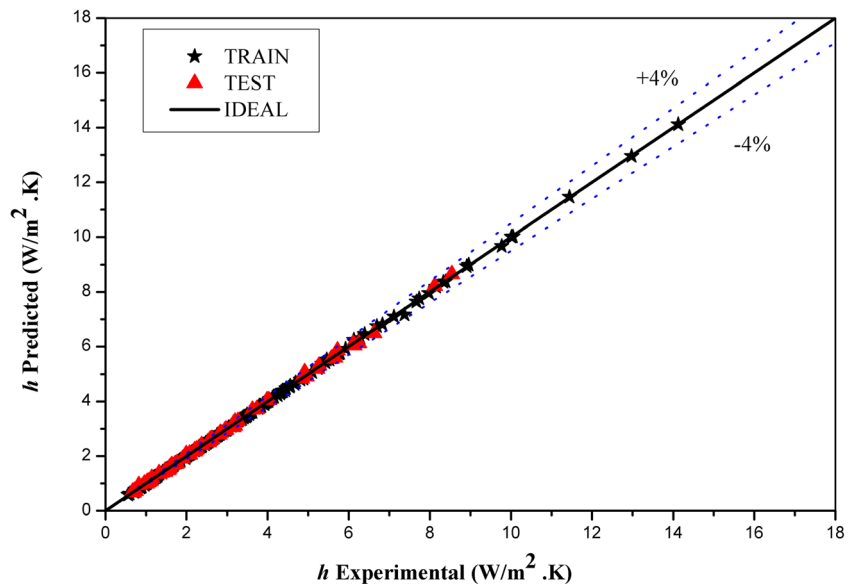
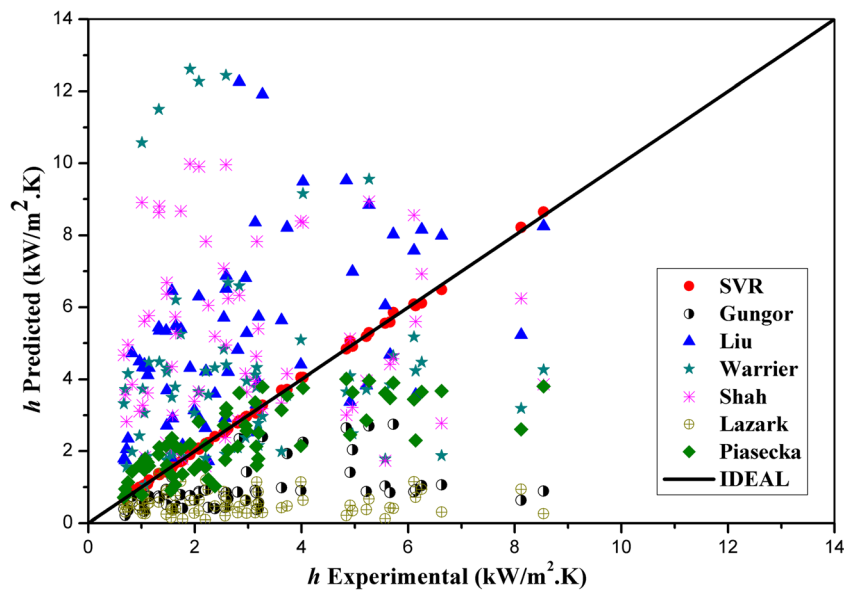


**Fig. 4** Comparison of SVR-based with the various correlations for predicting the subcooled flow boiling heat transfer coefficient,  $h$



[33]. The most commonly used kernel function is the Gaussian radial basis function (RBF) defined below:

$$K(x_i, x_j) = \exp\left(-\frac{\|x_i - x_j\|^2}{2\sigma^2}\right) \tag{8}$$

where,  $\sigma$  denotes the width of the RBF and

$$\gamma = \frac{1}{2\sigma^2} \tag{9}$$

Thus, the basic SVR function carries the following form:

$$f(x, \lambda_i, \lambda_i^*) = \sum_{i=1}^{N_{sv}} (\lambda_i - \lambda_i^*) K(x_i, x_j) + b \tag{10}$$

Karush-Kuhn-Tucker (KKT) conditions are used to compute the parameter,  $b$ , where the product between dual variables and constraints vanishes at the optimal solution.

### 3 Correlations for the flow boiling heat transfer

For evaluating the heat transfer coefficient in micro and mini-channels, eight different correlations given in literature have

been selected. Table 1 presents these selected correlations along with their respective range of applicability.

#### 3.1 SVR-based modeling procedure

The steps involved in the development of the SVR-based model are [43, 44]:

- Collection of data as independent and dependent variables
- Data preprocessing (normalization and scaling of data)
- Dividing the whole dataset into training and test dataset using simple random sampling technique (SRS)
- Selection of the appropriate kernel
- Optimizing the model parameters ( $C, \epsilon$ ) and kernel parameter ( $\gamma$ ) with grid search methodology and k-fold cross-validation.
- Model training with the optimum value of the model and kernel parameters ( $C, \epsilon, \gamma$ ).
- Evaluation of model performance in terms of statistical parameters such as average absolute relative error (AARE), root mean square error (RMSE), standard deviation (SD), mean relative error (MRE), leave-one-out

**Table 4** Comparison of SVR-based model with the existing subcooled correlations using test dataset

Correlations	AARE (%)	R	SD	Total error (%)	RMSE
SVR	1.71	0.9996	2.1585	±4	0.0244
Gungor & Winterton [35]	62.3	0.4449	2.6156	±92	3.4537
Liu & Winterton [39]	127.17	0.4847	2.4341	±367	0.5239
Warriar [41]	137.69	0.0703	2.7234	±560	0.6978
Shah [40]	170.2	0.13995	2.302	±564	0.6541
Lazark & Black [37]	72.31	0.1049	0.3004	±95	10.1096
Piasecka [42]	32.7	0.43797	37.46	±67	9.9876

**Table 5** Optimal parameters for the SVR-based model for predicting the saturated flow boiling heat transfer coefficient

Model	C	$\gamma = 1/2\sigma^2$	$\epsilon$	Kernel type	Type of loss function	Number of support vectors	Number of training points
Heat transfer coefficient, $h$	500	0.0528	0.0418	RBF	$\epsilon$ - insensitive	58	354

cross-validation on training dataset ( $Q_{Loo}^2$ ) and leave-one-out cross-validation on test dataset ( $Q_{ext}^2$ ).

## 4 Results and discussions

The flow boiling heat transfer coefficient for R-11 has been examined in a smooth copper tube with an inner diameter of

1.95 mm by Bao et al. [14]. They have performed the experiment over a wide range of parameters with heat flux ranging from 5 to 200 kW/m<sup>2</sup>; mass flux from 50 to 1800 kg/m<sup>2</sup> s, vapor qualities from 0 to 0.9, and system pressures from 0.2 to 0.5 MPa. Experiments performed by Bao et al. [14] have covered the whole saturated and subcooled boiling flow regime.

In this work, a comparative study of the existing correlations for flow boiling heat transfer in micro/mini-channels has been done. Furthermore, SVR-based models have been developed for predicting the flow boiling heat transfer coefficient in

**Fig. 5** **a** Training course curve for predicting the saturated flow boiling heat transfer coefficient,  $h$ . **b** Test course curve for predicting the saturated flow boiling heat transfer coefficient,  $h$

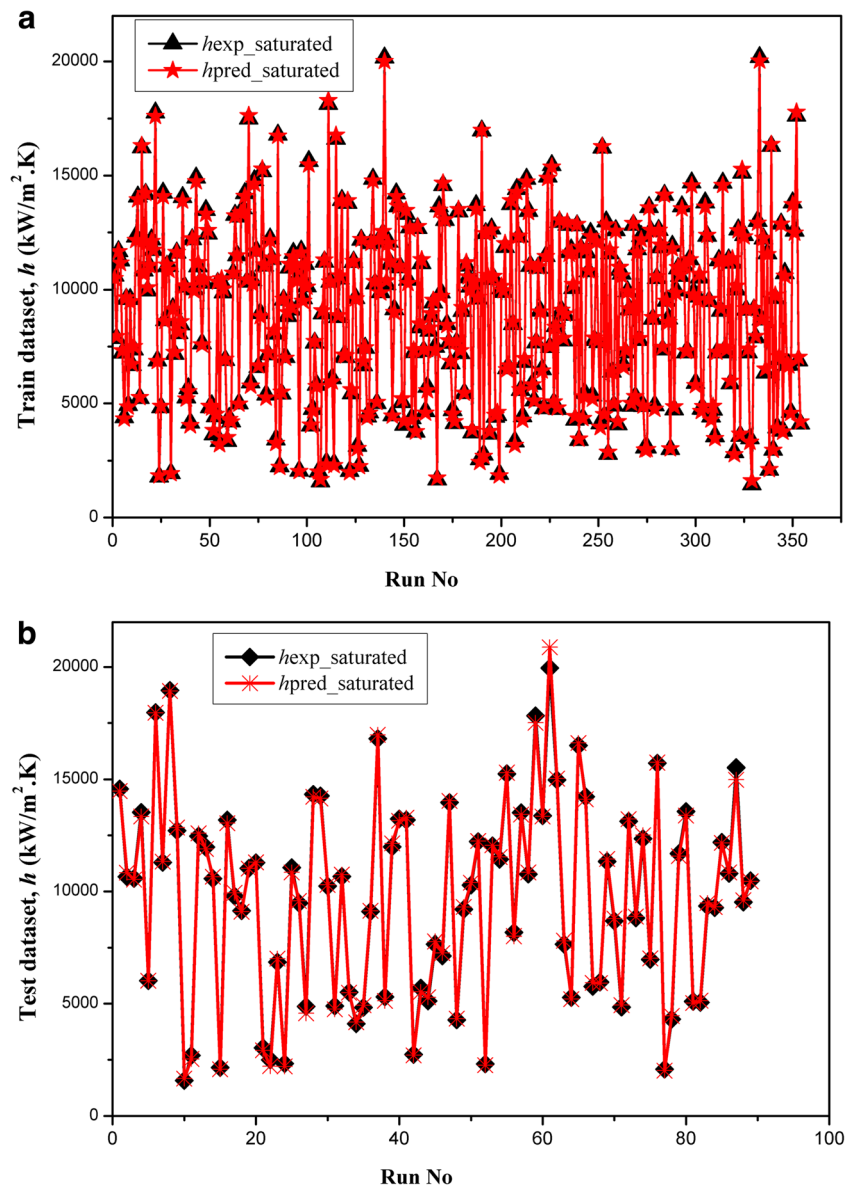
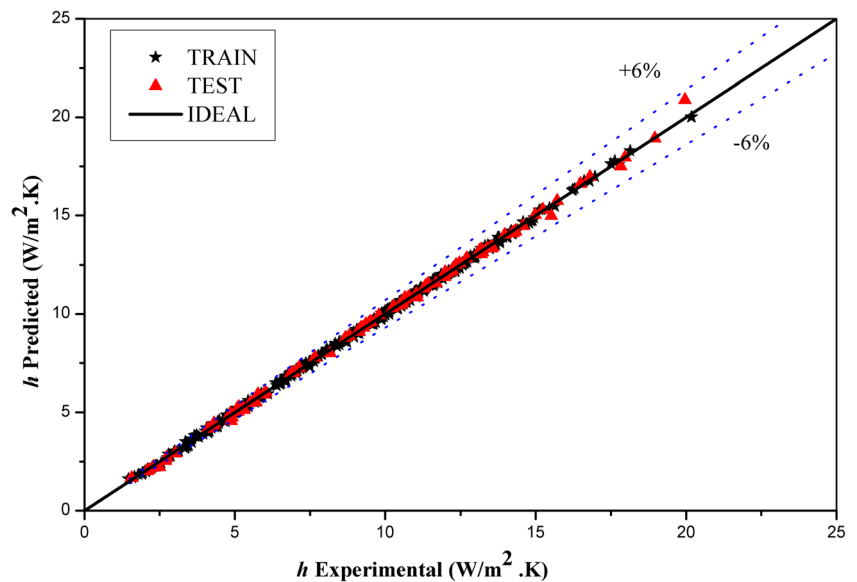




**Fig. 6** SVR simulation for predicting the saturated flow boiling heat transfer coefficient,  $h$  using optimal parameters for training dataset and test dataset



mini-channels for saturated and subcooled boiling, using the same dataset available from the published literature [14].

An SVR-implementation known as “ $\epsilon$ -SVR” in the software LIBSVM library [45] on MATLAB platform has been used to develop the SVR-based models. A comparison of the performance of the SVR-based models with the existing correlations has been carried out based on statistical parameters such as average absolute relative error (AARE), correlation coefficient (R) etc. Moreover, the SVR-based models have been used to predict the effect of various independent variables on the flow boiling heat transfer coefficient and comparison has been made with experimental data.

#### 4.1 Support vector regression-based model for subcooled flow boiling heat transfer

The whole dataset of 324 samples for subcooled boiling has been divided into the training dataset and the test dataset with simple random sampling (SRS) technique, as 80% (259 data points) and 20% (65 data points), respectively.

In the present work, the RBF kernel has been utilized as it requires only one parameter to be adjusted and has been found to give a good generalization performance than the other kernels [27]. Grid search methodology with 10-fold cross-validation has been used to obtain the optimal values of the SVR-based model and kernel parameters ( $C$ ,  $\epsilon$ , and  $\gamma$ ) by varying these parameters in a wide range of:  $C$  [ $2^5$ ,  $2^{15}$ ],  $\gamma$  [2–15, 22] and  $\epsilon$  [2–15, 24] on the training dataset. In this process the whole dataset has been partitioned into 10 equal parts. Thereafter, 9 parts have been used to develop the model for a fixed set of these parameters ( $C$ ,  $\epsilon$  and  $\gamma$ ) and each time the remaining one part has been utilized for validation (testing). The optimal parameters have been those which give the lowest mean squared error (MSE) [44, 46].

The value of regularization parameter  $C$  should not be too large as it can over-fit the data. On the other hand a small value of  $C$  increases the training error resulting in under-fitting and the model does not properly fit the learning data. A large value of epsilon  $\epsilon$  encloses a small number of support vectors (SVs) and thus results in more flat estimates (a low accuracy but simple model). On the other hand a small value of  $\epsilon$  has more data points lying outside the tube giving a large number of SVs. The kernel parameter gamma,  $\gamma$  in case of RBF kernel, is the inverse of standard deviation, which basically measures the similarity between two points. A small value of gamma means a large variance i.e. the chances of over-fitting increase. While a large value of gamma signifies a small variance resulting in under-fitting of the function [47]. Keeping these points in mind, the optimization procedure has been carried out. Table 2 gives the obtained optimal values of the SVR-based model parameters.

After obtaining the optimal values of the SVR parameters, training and test course curves for subcooled boiling have been constructed using training and test datasets as shown in Figs. 2a and b respectively.

**Table 6** SVR-based model evaluation based on statistical parameters for saturated boiling

Model Evaluation Indices For Saturated Boiling	Train data	Test data
AARE (%)	1.27	1.58
R	0.9997	0.9993
RMSE	0.0171	0.0243
SD	0.2066	0.2375
MRE	0.0126	0.0161
$Q^2_{\text{LOO}}$ (Train data), $Q^2_{\text{ext}}$ (Test data)	0.99989	0.99868

Figure 3 shows that the predicted values of the subcooled flow boiling heat transfer coefficient,  $h$  for the training data as well as the test data lie close to the ideal fit line and all the predicted data points lie within a total error of  $\pm 4\%$ . Table 3 exhibits the model evaluation parameters of the SVR-based model for both the training data as well as the test data during subcooled boiling. The obtained values of model evaluation parameters for the training data and test data reveal a high accuracy with excellent prediction performance of the SVR-based model.

#### 4.1.1 Comparative analysis of SVR-based model with the existing correlations for subcooled flow boiling heat transfer

There are some common correlations available in the literature, which can be applied to both subcooled and saturated boiling like Gungor & Winterton [35], Liu & Winterton [39], Warriar [41], Shah [40], Lazark & Black [37] and Piasecka [42]. A comparison has been made of the prediction performances of the SVR-based model with the existing correlations for the subcooled flow. Figure 4 gives the superior prediction performance of the SVR-based model. Table 4 exhibits the relevant model evaluation parameters for the SVR-based model and the correlations on the test dataset. The obtained results in Table 4 and Fig. 4 reveal that most of the correlations did not predict the flow boiling heat transfer coefficient very well, as opposed to the SVR-based model, which may again be attributed to the fact that they have been developed based on the empirical risk minimization (ERM) principle while the SVR-based model has been developed on the SRM principle. The SRM principle of SVR optimizes the generalization accuracy over the empirical error as well as the capacity of the machines or the

flatness of the model, while the ERM principle only minimizes the empirical error and does not take into account the model flatness. This results in overtraining i.e. high accuracy for training dataset and low for test dataset (unseen) giving poor generalization performance [25, 29]. The SVR-based model gives the highest prediction accuracy followed by Piasecka [42] and Gungor and Winterton [33].

#### 4.2 Support vector regression-based model for saturated flow boiling heat transfer

SVR-based model has also been developed for saturated boiling using the data from the literature [14]. Again, the whole dataset of saturated boiling with 443 samples has been partitioned into the training dataset and test dataset as 80% (354 data points) and 20% (89 data points), respectively. A similar procedure has been carried out for obtaining the optimal values of the SVR-based parameters ( $C$ ,  $\epsilon$ , and  $\gamma$ ). The finally obtained optimal values of the model parameters are given in Table 5. It has been observed that with 354 training data points, 58 SVs have been obtained. The lesser the number of SVs, the more sparse is the solution obtained.

After optimizing the SVR parameters, training and test course curves for saturated boiling have been constructed using training and test dataset as shown in Figs. 5a and b respectively.

The model output for the training and test dataset, between the experimental values of heat transfer coefficient  $h$  and those predicted by the SVR-based model, have been shown in Fig. 6. It is evident that both the predicted values for the training dataset as well as the test dataset lie close to the ideal fit line. Moreover, all the predicted data points lie within a total error of  $\pm 6\%$ . Table 6 exhibits the model

**Fig. 7** Comparison of SVR-based with the various correlations for predicting the heat transfer coefficient,  $h$  during saturated boiling

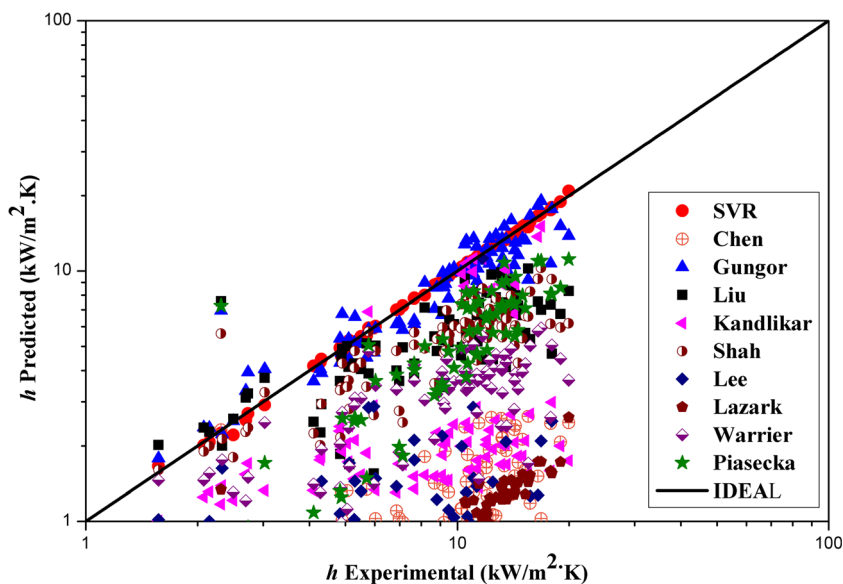


**Table 7** Comparison of the SVR-based model with the existing saturated boiling correlations over test dataset

Correlations	AARE (%)	R	SD	Total error (%)	RMSE
SVR	1.58	0.9993	0.2375	±6	0.0243
Chen [34]	85.02	0.6037	0.1986	±96	10.3478
Gungor & Winterton [35]	15.23	0.9062	0.2396	±40	0.2050
Liu & Winterton [39]	41.95	0.7136	0.2362	±73	0.9896
Kandlikar [36]	63.28	0.3485	0.2328	±91	4.0841
Shah [40]	40.95	0.7869	0.2362	±69	0.9724
Lee & Mudawar [38]	85.42	0.0630	0.2362	±93	29.1852
Lazark & Black [37]	90.47	0.9172	0.1866	±98	10.5046
Warrier [41]	62.65	0.6757	0.1338	±79	2.5858
Piasecka [42]	63.00	0.5651	1.4551	±83	37.57

evaluation parameters of the SVR-based model for both the training data as well as the test data. The close proximity to each other of the model evaluation parameters between the training dataset and test dataset testify to the excellent prediction performance of the SVR-based model and also to its high generalizability.

#### 4.2.1 Comparison of the SVR-based model with the existing correlations for saturated flow boiling heat transfer

Prediction performance of the SVR-based model has been compared with the existing saturated boiling correlations over an ideal fit line shown in Fig. 7. Table 7 exhibits the relevant model evaluation parameters for the SVR-based model and the correlations on the test dataset. The obtained results in Table 7 and Fig. 7 reveal that most of the correlations underpredict the flow boiling heat transfer coefficient. However, Gungor & Winterton [35], in particular, predicted the

experimental data with reasonable accuracy. The relatively poor performance of these correlations to predict the experimental data very well may be attributed to the fact that they are not general and have been developed for different flow conditions with different ranges. It can be easily surmised that the SVR-based model is an immensely improved model in comparison to the existing correlations.

#### 4.3 Parametric effects on flow boiling heat transfer coefficient

In this section, the effect of the various independent variables viz. vapor quality ( $x$ ), mass flux ( $G$ ), system pressure ( $P$ ), and heat flux ( $q$ ), on flow boiling heat transfer coefficient ( $h$ ) predicted by the SVR-based models are discussed in the light of the experimental results and the existing theory.

**Fig. 8** A plot of experimental and predicted heat transfer coefficient,  $h$  of R11 versus vapor quality,  $x$  at various mass flux (422 kPa inlet pressure; 58 kW/m<sup>2</sup> heat flux)

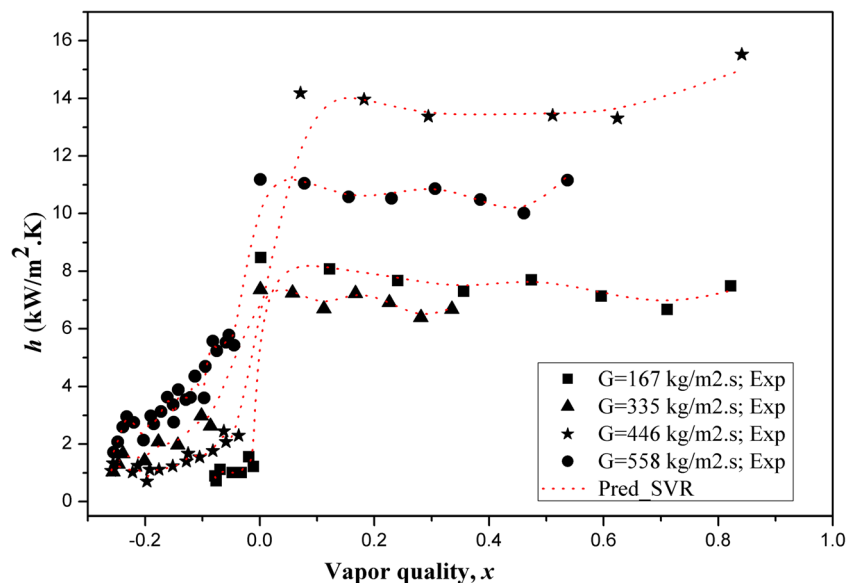
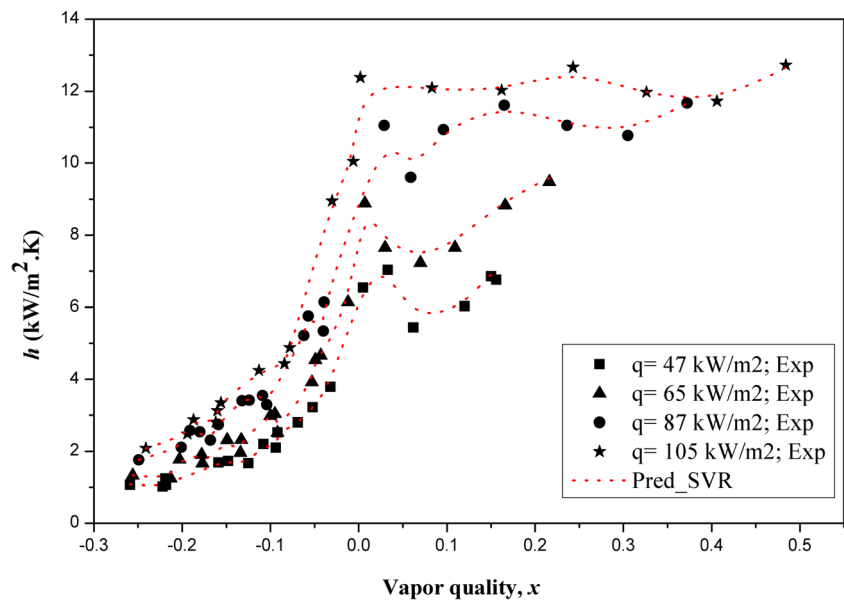


**Fig. 9** A plot of the experimental and the predicted heat transfer coefficient,  $h$  of R11 versus vapor quality,  $x$  for different heat fluxes (460 kPa inlet pressure; 446 kg/m<sup>2</sup>.s mass flux)



#### 4.3.1 The effect of mass flux and vapor quality on the flow boiling heat transfer coefficient

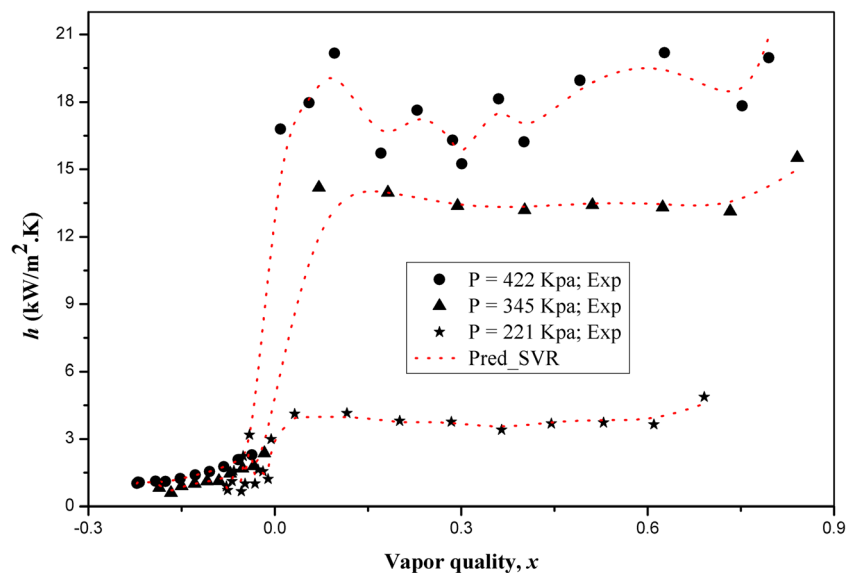
Figure 8 shows the experimentally determined heat transfer coefficient plotted against quality as a function of mass flux, at constant heat flux and system pressure. Quality,  $x$  within  $0 \leq x \leq 1$  corresponds to the saturated boiling while  $x < 0$  falls under the subcooled boiling region. Vapor quality,  $x$  for saturated region varies between 0.001 and 0.84, while heat transfer coefficient ranges from 4.35 up to 15.5 kW/m<sup>2</sup>.K. It is clear from the Fig. 8 that the heat transfer coefficient is independent of the mass flux and the vapor quality. This can be attributed to the fact that the heat transfer is dominated by nucleate boiling. Further, it has also been

observed that the predicted curve follows the same trend as that of the experimental results.

#### 4.3.2 The effect of heat flux on the flow boiling heat transfer coefficient

Figure 9 shows the experimental and predicted trend of heat transfer coefficient at a mass flux of 446.4 kg/m<sup>2</sup>.s at different values of heat flux. It has been observed that the heat flux,  $q$ , has a significant effect on heat transfer coefficient i.e. heat transfer coefficient increases with increasing the heat flux. The higher the heat flux, the higher the heat transfer coefficient [48]. The prediction performance of the SVR-based

**Fig. 10** A plot of the experimental and the predicted heat transfer coefficient,  $h$  of R11 versus vapor quality,  $x$ , at different pressures (heat flux is 120 kW/m<sup>2</sup> and the mass flux is 446 kg/m<sup>2</sup>.s)



models has been found to be in good agreement with the experimental results as is evident from Fig. 9.

#### 4.3.3 The effect of system pressure on the flow boiling heat transfer coefficient

The obtained experimental results in Fig. 10 have revealed that the heat transfer coefficient increases with increasing pressure. An increase in pressure causes variation in fluid properties such as decreasing surface tension and liquid-to-gas density ( $\rho_l/\rho_g$ ) which aids in the increase of the number of active nucleation sites [49]. It is, therefore, evident that the heat transfer coefficient in the nucleate boiling region is mainly affected by heat flux and pressure and is less sensitive to mass flux and vapor quality. It can be observed from Fig. 10 that the SVR-based models have faithfully predicted the experimental trends.

Thus, it can be confidently stated that the developed SVR-based models accurately depict the effect of the independent parameters like mass flux, vapor quality, heat flux and pressure on the flow boiling heat transfer coefficient of R11. This accuracy of the SVR-based models is attributed to SRM. That optimizes the generalization accuracy around the empirical error and the model flatness or the capacity of SVM.

## 5 Conclusions

In this paper, the application of SVR for the prediction of the flow boiling heat transfer coefficient of R11 in mini-channels has been presented. It has been found that the SVR prediction results are consistent with the experimental data. The simulation results have been compared with the well-established correlations found in the literature. It has been seen that the SVR-based models are far superior in performance to these correlations. Among the existing correlations, the predictions of heat transfer coefficient by Gungor and Winterton [35] and Piasecka [42] are the most accurate. The SVR-based models were also tested for analyzing the effects of mass flux, vapor quality, heat flux and pressure on the flow boiling heat transfer coefficient in the subcooled boiling and the saturated boiling regions. It was found that the SVR-based model faithfully and accurately followed the same trend as depicted by the experimental data with respect to all the independent parameters such as mass flux, vapor quality, heat flux, and pressure, with high accuracy. This high accuracy can be attributed to the structural risk minimization (SRM) principle on which SVR is based.

**Acknowledgments** Authors sincerely extend their thanks and gratitude to Messrs. Z.Y. Bao, D.F. Fletcher and B.S. Haynes for the availability of their published work from which the flow boiling heat transfer data has been retrieved for model formulation and validation. Authors also want to acknowledge Messrs. N.O. Olayiwola and S.M. Ghiaassian from whom we got the motivation for carrying out the present research.

**Publisher's Note** Springer Nature remains neutral with regard to jurisdictional claims in published maps and institutional affiliations.

## References

- Rao M, Khandekar S (2009) Simultaneously Developing Flows Under Conjugated Conditions in a Mini-Channel Array: Liquid Crystal Thermography and Computational. *Heat Transf Eng* 30: 751–761. <https://doi.org/10.1080/01457630802678573>.
- Thakkar K, Kumar K, Trivedi H (2014) Thermal & Hydraulic Characteristics of Single phase flow in Mini-channel for Electronic cooling – Review. *Int J Innov Res Sci Eng Technol* 3: 9726–9733
- Kandlikar SG (2002) Fundamental issues related to flow boiling in minichannels and microchannels. *Exp Thermal Fluid Sci* 26:389–407. [https://doi.org/10.1016/S0894-1777\(02\)00150-4](https://doi.org/10.1016/S0894-1777(02)00150-4)
- Joshi LC, Singh S, Kumar SR (2014) A review on enhancement of heat transfer in microchannel heat exchanger. *Int J Innov Sci Eng Technol* 1:529–535
- Qu W, Mudawar I (2003) Flow boiling heat transfer in two-phase micro-channel heat sinks -I. Experimental investigation and assessment of correlation methods. *Int J Heat Mass Transf* 46:2755–2771. [https://doi.org/10.1016/S0017-9310\(03\)00041-3](https://doi.org/10.1016/S0017-9310(03)00041-3)
- Copetti JB, Zinani F, Ayres FGB, Schaefer F (2015) Boiling heat transfer in Mini Tube: A discussion of two phase heat transfer coefficient behaviour, flow patterns and heat transfer correlations for two refrigerants, IV Journeys Multiph. *Flows (JEM 2015)*, 1–9
- Li W, Wu Z (2010) A general criterion for evaporative heat transfer in micro/mini-channels. *Int J Heat Mass Transf* 53:1967–1976. <https://doi.org/10.1016/j.ijheatmasstransfer.2009.12.059>
- Xiande F, Rongrong S, Zhanru Z (2011) Correlations of Flow Boiling Heat Transfer of R-134a in Minichannels : Comparative study. *Energy Sci Technol* 1:1–15
- Piasecka M (2014) Application of heat transfer correlations for FC-72 flow boiling heat transfer in minichannels with various orientations. *MATEC Web Conf* 18:1–8
- Mahmoud MM, Karayiannis TG (2013) Heat transfer correlation for flow boiling in small to micro tubes. *Int J Heat Mass Transf* 66: 553–574
- Basu S, Ndao S, Michna GJ, Jensen MK (2011) Flow Boiling of R134a in Circular Microtubes -Part I: Study of Heat. *J Heat Transf* 133:051502–051509. <https://doi.org/10.1115/1.4003159>.
- Olayiwola NO (2005) Boiling in Mini and Micro-Channels. M. S. Thesis, School of mechanical Engineering, Georgia Institute of Technology, Atlanta
- Olayiwola NO, Ghiaassian SM (2006) Assessment of flow boiling heat transfer correlations for application to mini-channels. In: 2006 ASME Int. Mech. Eng. Congr. Expo., ASME, Chicago, pp. 1–16
- Bao ZY, Fletcher DF, Haynes BS (2000) Flow boiling heat transfer of Freon R11 and HCFC123 in narrow passages. *Int J Heat Mass Transf* 43:3347–3358. [https://doi.org/10.1016/S0017-9310\(99\)00379-8](https://doi.org/10.1016/S0017-9310(99)00379-8)
- Baird JR, Bao ZY, Fletcher DF, Haynes BS (2000) Local flow boiling heat transfer coefficients in narrow conduits. *Multiph Sci Technol* 12:129–144. <https://doi.org/10.1615/MultScienTechn.v12.i3-4.80>
- Yan Y-Y, Lin T-F (1998) Evaporation heat transfer and pressure drop of refrigerant R-134a in a small pipe. *Int J Heat Mass Transf* 41:4183–4194
- Peng H, Ling X (2015) Predicting thermal-hydraulic performances in compact heat exchangers by support vector regression. *Int J Heat Mass Transf* 84:203–213. <https://doi.org/10.1016/j.ijheatmasstransfer.2015.01.017>.

18. Zaidi S (2012) Development of support vector regression (SVR)-based model for prediction of circulation rate in a vertical tube thermosiphon reboiler. *Chem Eng Sci* 69:514–521. <https://doi.org/10.1016/j.ces.2011.11.005>.
19. Shabri A, Suhartono (2012) Streamflow forecasting using least-squares support vector machines. *Hydrol Sci J* 57:1275–1293. <https://doi.org/10.1080/02626667.2012.714468>
20. Bui Tien D, Pham BT, Nguyen QP, Hoang N-D (2016) Spatial prediction of rainfall-induced shallow landslides using hybrid integration approach of Least-Squares Support Vector Machines and differential evolution optimization: a case study in Central Vietnam. *Int J Digit Earth* 9:1077–1097. <https://doi.org/10.1080/17538947.2016.1169561>
21. Thissen U, Van Brakel R, De WP, Melssen WJ, Buydens LMC (2003) Using support vector machines for time series prediction. *Chemom Intell Lab Syst* 69:35–49. [https://doi.org/10.1016/S0169-7439\(03\)00111-4](https://doi.org/10.1016/S0169-7439(03)00111-4)
22. Burbidge R, Trotter M, Buxton B, Holden S (2001) Drug design by machine learning : support vector machines for pharmaceutical data analysis. *Comput Chem* 26:5–14
23. Parveen N, Zaidi S, Danish M (2016) Support vector regression model for predicting the sorption capacity of lead (II). *Perspect Sci* 8:629–631
24. Parveen N, Zaidi S, Danish M (2017) Support Vector Regression Prediction and Analysis of the Copper (II) Biosorption Efficiency. *Indian Chem Eng* 59:295–311. <https://doi.org/10.1080/00194506.2016.1270778>
25. Vapnik V, Golowich SE, Smola A (1996) Support Vector Method for Function Approximation, Regression Estimation, and Signal Processing. *Adv Neural Inf Proces Syst* 9:281–287
26. Gunn S (1997) Support Vector Machines for Classification and Regression, ISIS Technical Report. University of Southampton, Southampton, pp 1–42
27. Zaidi S (2015) Novel application of Support Vector Machines to model the two phase-boiling heat transfer coefficient in a vertical tube thermosiphon reboiler. *Chem Eng Res Des* 98:44–58. <https://doi.org/10.1016/j.saa.2011.10.074>.
28. Parveen N, Zaidi S, Danish M (2017) Development of SVR-based model and comparative analysis with MLR and ANN models for predicting the sorption capacity of Cr(VI). *Process Saf Environ Prot* 107:428–437. <https://doi.org/10.1016/j.psep.2017.03.007>.
29. Vapnik VN (1995) *The Nature of Statistical Learning Theory*. Springer, New York
30. Pan Y, Jiang J, Wang R, Cao H, Cui Y (2009) Predicting the auto-ignition temperatures of organic compounds from molecular structure using support vector machine. *J Hazard Mater* 164:1242–1249. <https://doi.org/10.1016/j.jhazmat.2008.09.031>.
31. Sriraam A, Sekar S K, Samui P (2012) Support Vector Machine Modelling for the Compressive Strength of Concrete. In: B.H.V. Topping (Ed.), *Proc. Eighth Int. Conf. Eng. Comput. Technol., Civil-Comp Press, Scotland*, pp. 1–15
32. Nachev A, Stoyanov B (2012) Product quality analysis using support vector machines. *Int J Inf Model Anal* 1:179–192
33. Smola AJ, Schölkopf B (2004) A tutorial on support vector regression. *Stat Comput* 14:199–222. <https://doi.org/10.1023/B:STCO.0000035301.49549.88>
34. Chen JC (1966) Correlation for boiling heat transfer to saturated fluids in convective flow. *Ind Eng Chem Process Des Dev* 5:322–329
35. Gungor KE, Winterton RHS (1987) Simplified general correlation for saturated flow boiling and comparison with data. *Chem Eng Res Des* 65:148–156
36. Kandlikar S G, (1990) Flow boiling maps for water, R-22 and R-134a in the saturated region. In: *Int. Heat Transf. Conf., Jerusalem*, pp. 1–6
37. Lazarek GM, Black SH (1982) Evaporative heat transfer, pressure drop and critical heat flux in a small vertical tube with R-113. *Int J Heat Mass Transf* 25:945–960
38. Lee J, Mudawar I (2005) Two-phase flow in high-heat-flux micro-channel heat sink for refrigeration cooling applications: Part II — heat transfer characteristics. *Int J Heat Mass Transf* 48:941–955. <https://doi.org/10.1016/j.ijheatmasstransfer.2004.09.019>
39. Liu Z, Winterton RHS (1991) A general correlation for saturated and subcooled flow boiling in tubes and annuli , based on a nucleate pool boiling equation. *Int J Heat Mass Transf* 34:2759–2766
40. Mohammad PE, Shah M (1982) Chart correlation for saturated boiling heat transfer : Equations and further study. *ASHRAE Trans* 88:185–196
41. Warriar GR, Dhir VK, Momoda LA (2002) Heat transfer and pressure drop in narrow rectangular channels. *Exp Thermal Fluid Sci* 26:53–64
42. Piasecka M (2015) Correlation for flow boiling heat transfer in minichannels with various orientations. *Int J Heat Mass Transf* 81:114–121
43. Shi XZ, Zhou J, Wu BB, Huang D, Wei W (2012) Support vector machines approach to mean particle size of rock fragmentation due to bench blasting prediction. *Trans Nonferrous Metals Soc China* 22:432–441. [https://doi.org/10.1016/S1003-6326\(11\)61195-3](https://doi.org/10.1016/S1003-6326(11)61195-3)
44. Lee C-Y, Chern S-G (2013) Application of a Support Vector Machine for Liquefaction Assessment. *J Mar Sci Technol* 21: 318–324. <https://doi.org/10.6119/JMST-012-0518-3>.
45. Chang C-C, Lin C-J (2011) A Library for Support Vector Machines, *ACM Trans. Interlligent Syst. Technology* 2:1–27. <https://doi.org/10.1145/1961189.1961199>
46. Jung Y (2018) Multiple predicting  $K$ -fold cross-validation for model selection. *J Nonparametr Stat* 30:197–215. <https://doi.org/10.1080/10485252.2017.1404598>
47. Chang Q, Chen Q, Wang X (2005) Scaling Gaussian RBF kernel width to improve SVM classification. In: *Int. Conf. Neural Networks Brain, 2005 ICNN, Beijing*
48. Bertsch SS, Groll EA, Garimella SV (2009) Effects of heat flux, mass flux, vapor quality, and saturation temperature on flow boiling heat transfer in microchannels. *Int J Multiphase Flow* 35:142–154. <https://doi.org/10.1016/j.ijmultiphaseflow.2008.10.004>
49. Yan J, Bi Q, Liu Z, Zhu G, Cai L (2015) Subcooled flow boiling heat transfer of water in a circular tube under high heat fluxes and high mass fluxes. *Fusion Eng Des* 100:406–418. <https://doi.org/10.1016/j.fusengdes.2015.07.007>.